

Theoretical Calculations of
Peripheral Reaction Yields
from Relativistic Heavy Ions*

John Rasmussen, Raul Donangelo,
and Luiz Oliveira

Nuclear Science Division, Lawrence
Berkeley Laboratory, University of California
Berkeley, California 94720

NOTICE
This report was prepared as an account of work sponsored by the United States Government. Neither the United States nor the United States Energy Research and Development Administration, nor any of their employees, nor any of their contractors, subcontractors, or their employees, makes any warranty, express or implied, or assumes any legal liability or responsibility for the accuracy, completeness or usefulness of any information, apparatus, product or process disclosed, or represents that its use would not infringe privately owned rights.

Paper to be presented at Hakone (Japan)
Meeting on Nuclear Reactions Sept. 2-3, 1977

*This work carried out under auspices of the U.S. Energy Research and Development Administration.

In this paper we direct attention mainly toward interpreting the experimental results of Shibata et al¹ with 250 MeV/N and 400 MeV/N carbon ions and alpha particles on calcium targets at the Berkeley BEVALAC. Some of these results are summarized in Figs. 1 and 2. Cross sections for odd products may scatter, since these are particular gamma transition yields. The even-even points are more representative of full isotopic yield, since they are mostly based on $2 + 0(\text{gd})$ transitions. Only relative yields were measured at 250 MeV/N, and they fall off more steeply with Q_{\min} than those at 400 MeV/N, the characteristic $1/e$ fall-off being 10 MeV at 250 MeV/N and 17 MeV at 400 MeV/N.

We have drawn on the works of D. Bowman and W. Swiatecki² and of Hufner et al³ that was directed toward understanding the ^{16}O projectile fragmentation cross sections at 1 and 2 GeV/N. We take note also of the calculations of Loveland et al⁴ on product yields in the gold region following relativistic carbon bombardment of uranium.

The mass-40 region we address is of special interest in that geometrical and statistical models for the fast process and the subsequent evaporation stage should be more applicable than for the light projectile fragmentation. In contrast to the heavy element region we have no fission competition, and alpha evaporation is a significant process. There are also available considerable other data on ^{40}Ca targets excited by high energy protons⁵ and by pions⁶, though we shall not have space here to consider them in detail.

For the fast process we have used two related but different models, Swiatecki's abrasion (fireball) model and Myers' firestreak model.

In the abrasion model one calculates geometrically as a function of impact parameter, b , the volume fractions f_T and f_p remaining in the spectator pieces of target and projectile, respectively. From the inverse function $b(f_T)$ the partial cross section for a primary fragment of mass A is determined as

$$\sigma(A) = \pi \left[b \left(\frac{A+0.5}{A_T} \right)^2 - b \left(\frac{A-0.5}{A_T} \right)^2 \right]$$

In our calculations we introduce a dispersion in charge to mass ratio much as did Hufner. That is, each struck target nucleon is assumed to have a Z/A probability of being a proton. Hence, the charge dispersion for constant A has the form of a hypergeometric distribution

$$P(z,n) = \frac{\binom{Z}{z} \binom{N}{n}}{\binom{A}{a}} ,$$

where the capitals refer to the target nucleus and lower case letters refer to the knocked-out protons z , neutrons n , and total nucleons $a (=z+n)$, respectively.

Before beginning the evaporation calculations to determine final products, it is necessary to specify an excitation energy distribution for the primary fragments. Swiatecki proposed an excitation energy term equal to the excess surface energy of the abrasion product, and we calculate and include this term. Following Hufner

we also add a final state interaction, assuming each struck nucleon has a 50% chance of passing through the spectator and depositing 40 MeV of excitation. (This energy value, the dominance of (N,N), and the balancing out of capture against (N, 2N) processes can be rationalized from Monte Carlo work of Metropolis et al.⁷) Thus, each primary spectator with A-a mass number has a final state interaction with a number of nucleons m_{FSI} which have a binomial distribution given by

$$\text{Prob} \left(m_{FSI} \right) = \frac{\binom{a}{m_{FSI}}}{2^a} \quad (3)$$

The excitation energy is given, for each m_{FSI} , by

$$E_{FSI} = 40 m_{FSI} \quad (3')$$

With the primary fragment Z, N, and E distributions from the fast process determined we begin calculation of the statistical evaporation of nucleons, deuterons, and alpha particles using Blann's code ALICE⁸ as a subroutine. We use his options of Myers-Swiatecki shell-corrected formula masses and level density constant $a = A/8 \text{ MeV}^{-1}$. We assume zero angular momentum throughout the evaporation cascades, since it is not obvious how to calculate spin distributions in the fast process and they may well be generally small.

The abrasion model calculations, which are independent of bombarding energy, are shown in Table 1 alongside the 400 MeV/N experimental cross sections. (We show experimental cross sections only for the even products from $2 \rightarrow 0(\text{gd})$ transitions.) The fit for the principal products derived by multiple alpha removal from

^{40}Ca is reasonable. However, there are two shortcomings that impel us to look to more refined model calculations. First, there is the lack of bombarding energy dependence of the abrasion model. Second, there is the feature that the abrasion model implies a strong correlation between target spectator excitation and projectile spectator excitation. The smaller the impact parameter the greater this excitation. Photographic emulsion experiments of Heckman's group⁹ have shown, however, the presence of considerable pure target or pure projectile fragmentation events (some 7 to 16% of each with nitrogen and oxygen beams at 2 GeV/N). Furthermore, there are the correlation experiments of Crawford et al¹⁰ between sodium target gamma rays and carbon beam fragmentation patterns at 400 MeV/N. These results suggest very little correlation between the fates of the two collision partners, approaching the particle-physics limiting factorization behavior. This near factorization necessitates in addition to abrasion a grazing "Stochastic" excitation mechanism in which internal degrees of freedom of each collision partner independently extract translational energy through the time-dependent field of the other nucleus.

To bring a greater measure of sophistication to the fast process we have gone on to explore the "firestreak" model of Myers. In this model the collision is subdivided into a set of "tubes" parallel to the relative velocity vector, with the matter within each tube assumed to thermally equilibrate all energy in excess of the translational kinetic energy for momentum-conserving center-of-mass motion of the tube. In order to divide the tubes between

spectators and escaping firestreak it is necessary to specify some critical tube momentum p_c above which the tube escapes from the spectator. Clearly there will be a dependence on bombarding energy in the relationship between impact parameter and spectator mass. We have performed the firestreak calculation for several values of the critical momentum p_c/p_{Fermi} (0.2, 0.45, and 1.0). These p_c values correspond respectively to tube translational energies of 1 MeV/N, 8 MeV/N, and 38 MeV/N. The results are listed in Table I, where the firestreak calculations are denoted by 1, 2, and 3, respectively. The first case with $p_c/p_{\text{F}} = 0.2$ should approach the abrasion model calculation, since tubes with even slight overlap with projectile matter are ejected. It is evident from Table I that the cross sections of abrasion and firestreak 1 well agree.

With the firestreak model, especially cases 2 and 3, there is an additional term contributing to the spectator excitation besides the extra-surface term and the FSI. That is, those tubes receiving less than the critical momentum p_c for knock-out contribute their total projectile energy input. Table II shows for some of the reaction intermediates (before final state interaction) their partial formation cross sections and excitation energies. From the abrasion model values one can see the surface energy term alone, and the extra excitation energy in the firestreak calculations arises from the "retained tubes."

Let us turn to consider the grazing "stochastic" excitation mechanism mentioned earlier. It has been shown by Boisson et al¹² (eq. 12) that the time-dependent nuclear potential energy felt at

the nearest point on the target surface during a grazing collision has a Gaussian dependence on time near time zero

$$V(t) \propto \exp(-t^2/t_0^2), \text{ where}$$

$t_0 = [2 r_0 (R_t + R_p)]^{1/2}/v$, with R_t and R_p the radii of target and projectile nuclei, r_0 the range of the interaction and v speed of the projectile. The relativistic modification would replace v by $c\beta/\sqrt{1-\beta^2}$. In general terms the nucleus is exposed to a perturbing field with energy (frequency) spectrum a Gaussian, the Fourier transform of $V(t)$. That is, the characteristic energy $E_0 = 2 h/t_0$. For $^{12}\text{C} + ^{40}\text{Ca}$ with force range and radius constant 1.4 Fm we get $E_0 = 83 \beta/\sqrt{1-\beta^2}$ MeV, which gives 85 MeV at 400 MeV/N and gives 65 MeV at 250 MeV/N. The actual nuclear excitation spectrum will depend on various nuclear strength functions, most likely the isoscalar multipoles, quadrupole, octupole and higher. For orientation purposes if we assume flat nuclear strength functions, the stochastic grazing process would leave the ^{40}Ca target with a Gaussian distribution of excitation energy with the above widths (85 MeV or 65 MeV respectively). It may be that the nuclear strength function falls off with characteristic Fermi energy if particle-hole excitation is the main mode of energy absorption. In that case the 85 and 65 MeV figures might be reduced.

The total cross section involved in the stochastic process may be estimated from the emulsion studies cited. About one tenth of observed heavy-ion events are pure target fragmentation, and the contributing range of impact parameters should be of the order of the force range of ~ 1.4 Fm. Then we can be consistent with emulsion

observations if we say there is an 0.5 probability of a quantum of excitation being absorbed in this grazing zone, for then the $1.4 \times 2\pi \times (R_t + R_p)$ rim cross section of 0.70 barns divides into 4 equal parts, (1) pure target excitation, (2) pure projectile excitation, (3) both excited, and (4) neither excited. The 0.70/4 (≈ 0.175 barns) to each process is only slightly less than 10% of the geometrical cross section $(R_t + R_p)^2$ of ≈ 2.00 barns.

Table 3 lists the percentage yields expected for various products from the Gaussian excitation energy distribution in ^{40}Ca from the stochastic grazing process.

We do not have at this time a fully satisfactory theoretical explanation of the results of Shibata et al.¹. We prefer firestreak 2 plus the stochastic grazing process, although the total theoretical cross sections generally exceed those measured. The absolute normalization of the experimental cross sections is less certain than the determination of relative cross sections. We are looking forward to comparison with beam fragmentation data from various s-d shell nuclei and ^{56}Fe in unpublished experimental studies of Lindstrom et al.¹³.

As it affects these calculations, the firestreak model at low critical momentum p_c for knock out (calculations 1 and 2) is not very different from the simpler abrasion (fireball) model, and the latter might continue to be used.

There is much yet to be done, and we hope the present work helps define the questions for further studies. Our lack of

agreement with data may indicate the need to modify the cylindrical scraping geometries of abrasion and firestreak models to allow for lateral spreading of a fast cascade bounded by conical surfaces.

Acknowledgements

We are most grateful to Marshall Blann for making the ALICE code available and to Bill Myers for generously giving and helping us adapt key portions of his firestreak code. Wladek Swiatecki, Walter Loveland, and Roland Otto generously helped and made available the abrasion model code.

Various members of the TOSABE (Tokyo, Berkeley, Osaka) group have contributed significantly to development of the concepts behind these calculations, notably K. Nakai, T. Shibata, H. Ejiri, J. Ioannou, and J. Chiba.

References

1. T. Shibata et al, Contribution to the International Conference on Nuclear Structure - Tokyo (1977).
2. J. D. Bowman, W. J. Swiatecki and C. F. Tsang, LBL Report 2908 (1973).
3. J. Hufner, K. Schäfer and B. Schürmann, Phys. Rev. C, 12 (1975) 1888.
4. W. Loveland et al, Phys. Rev. Lett. 39, 320 (1977).

5. O. Artun et al, Phys. Rev. Lett. 35 (1975) 773.
6. H. E. Jackson et al, Phys. Rev. Lett. 35 (1975) 1170.
7. N. Metropolis et al, Phys. Rev. 110 (1958) 185.
8. M. Blann, "OVERLAID ALICE", COO-3494-29, Rochester University Report.
9. H. H. Heckman et al, "An Atlas of Heavy Ion Fragmentation Topology" - Unpublished.
10. H. J. Crawford et al, Bull. Am. Phys. Soc., 22 (1977) 594.
11. W. D. Myers, Private Communication (1977).
12. J. P. Boisson et al, LBL Report 5814 (1976).
13. P. J. Lindstrom, Private Communication (1977).

Table I. Cross Sections (mb) of Reaction Products (even-even only) from
 $^{12}\text{C} + ^{40}\text{Ca}$ Collisions Excluding Stochastic Grazing Process

	Exp. (2+0 γ -ray)	Abrasion Ablation	$E_{\text{LAB}} = 400.$ MeV/N			$E_{\text{LAB}} = 250.$ MeV/N		
			Firestreak 1	Firestreak 2	Firestreak 3	Firestreak 1	Firestreak 2	Firestreak 3
^{40}Ca	$14.4 \pm 3.8^{\text{a}}$	-	-	-	-	-	-	-
^{38}Ca	5.7 ± 2.8	7.7	7.7	-	-	7.8	-	-
^{38}Ar	15.2 ± 3.5	7.8	7.7	7.8	-	7.8	50.7^{d}	-
^{36}Ar	$\leq 38.6 \pm 6.2^{\text{b}}$	40.7	43.8	39.2	38.8	44.1	32.1	-
^{34}S	13.2 ± 6.0	28.8	25.8	23.7	27.3	27.5	25.0	-
^{32}S	$\leq 23.5 \pm 5.1^{\text{c}}$	32.0	31.9	30.7	12.4	32.9	29.4	3.1
^{32}Si	7.7 ± 2.2	1.6	1.9	1.8	0.9	1.9	1.7	0.4
^{30}Si	$\leq 23.5 \pm 5.1^{\text{c}}$	21.5	22.0	23.6	19.6	22.0	24.1	8.0
^{28}Si	22.0 ± 4.5	24.1	24.6	24.1	33.7	24.6	25.0	23.1
^{26}Mg	16.5 ± 3.9	16.2	16.7	17.0	12.2	16.4	17.3	22.2
^{24}Mg	20.5 ± 5.7	25.0	25.9	25.9	22.6	26.0	25.8	32.6
^{22}Ne	7.6 ± 2.6	9.3	11.0	10.8	5.3	11.0	10.6	-

a. $3 \rightarrow 0^+$ (g.s.) transition

b. Gamma unresolved from transition in ^{33}Si ; 38.6 mb is total.

c. Gammas unresolved for ^{32}S and ^{30}Si ; 23.5 mb is total.

d. This large cross section compared to its 400 MeV/N value shows the sensitivity of cross sections near the target mass to the discrete excitation energy chosen.

The primary ^{39}K intermediate is excited just above the proton binding energy for 250 MeV/N and just below for 400 MeV/N.

Table II. Firestreak 2 Cross Sections and Excitation Energies
(excluding FSI Energy) for Fast Stage Products
of Given A.

Mass No. A	Firestreak 2 at 400 MeV/N		Firestreak at 250 MeV/N		Abrasion	
	σ (mb)	$E^*(\text{MeV}) =$ $E_{\text{surf}} + E_{\text{tubes}}$	σ (mb)	$E^*(\text{MeV}) =$ $E_{\text{surf}} + E_{\text{tubes}}$	σ (mb)	$E^*(\text{MeV}) =$ E_{surf}
39	193	5.8	203	8.1	193	1.5
38	128	10.2	128	13.6	126	5.0
37	107	17.9	101	19.3	99	8.7
36	84	25.2	83	26.4	83	12.6
35	72	32.1	71	31.5	72	16.7
34	62	37.2	63	38.2	63	21.0
33	55	41.7	59	44.3	56	25.6
32	51	47.1	51	51.5	51	30.3
31	46	52.9	45	57.9	46	35

Table III. Percentage of various evaporation products from excited ^{40}Ca

Product	E ₀ (MeV)				
	25	45	65	85	105
^{40}Ca	42.9	24.7	17.2	13.2	10.8
^{39}Ca	1.7	1.7	1.4	1.1	0.9
^{38}Ca	0.1	0.3	0.3	0.3	0.3
^{39}K	29.7	21.6	16.0	12.5	10.3
^{38}K	1.1	2.0	1.8	1.5	1.3
^{37}K	—	0.4	0.5	0.4	0.4
^{38}Ar	9.3	13.1	11.5	9.7	8.2
^{37}Ar	0.6	3.8	4.6	4.4	4.0
^{36}Ar	8.3	9.2	8.8	7.9	7.0
^{35}Ar	0.3	1.0	1.1	1.1	1.0
^{37}Cl	0.1	0.9	1.1	1.1	1.0
^{36}Cl	—	0.2	0.4	0.4	0.4
^{35}Cl	3.4	6.3	6.8	6.4	5.8
^{34}Cl	—	0.7	1.1	1.2	1.2
^{34}S	0.6	4.9	6.8	7.3	7.0
^{33}S	—	1.1	2.9	3.7	4.0
^{32}S	0.7	2.3	4.1	5.1	5.4
^{31}P	—	1.3	2.4	3.5	3.9
^{30}Si	—	0.4	1.7	2.7	3.5
^{28}Si	—	0.4	1.0	2.3	3.3
^{27}Al	—	—	0.4	0.8	1.5
^{26}Mg	—	—	0.2	0.6	1.1
^{24}Mg	—	—	0.2	0.5	1.2

Table IV: Cross Sections (>1.0 mb) for all Products

Z	A	250. MeV/N			400. MeV/N		
		FIRESTREAK 2	STOCHASTIC $E_o = 65$ MeV	TOTAL	FIRESTREAK 2	STOCHASTIC $E_o = 85$ MeV	TOTAL
20	40	-	60.2	60.2	-	46.2	46.2
20	39	50.7	4.9	55.6	48.2	3.8	52.0
20	38	-	1.0	1.0	-	1.0	1.0
19	39	-	56.0	56.0	48.2	43.8	92.0
19	38	-	6.3	6.3	-	5.4	5.4
19	37	8.8	1.8	10.6	8.1	1.5	9.6
18	38	50.7	40.3	91.0	7.8	34.0	41.8
18	37	19.7	16.1	35.8	19.8	15.4	35.2
18	36	32.1	30.8	62.9	39.2	27.7	66.9
18	35	3.7	3.9	7.6	4.2	3.9	8.1
17	37	4.3	3.9	8.2	1.1	3.8	4.9
17	36	5.9	1.4	7.3	5.9	1.4	7.3
17	35	19.7	23.8	43.5	16.0	22.2	38.2
17	34	4.4	3.9	8.3	4.2	4.2	8.4
17	33	8.5	1.3	9.8	7.8	1.7	9.5
16	36	3.8	1.0	4.8	3.8	1.1	4.9
16	35	1.7	0.4	2.1	1.9	0.6	2.5
16	34	25.0	23.9	48.9	23.7	25.5	49.2
16	33	29.4	10.1	39.5	29.1	12.9	42.0
16	32	29.4	14.4	43.8	30.7	17.8	48.5
16	31	4.7	1.6	6.3	4.8	2.3	7.1
16	30	3.3	0.6	3.9	3.1	0.9	4.0
15	33	4.3	1.2	5.5	4.1	1.6	5.7
15	32	2.8	0.5	3.3	2.6	0.9	3.5
15	31	19.8	8.4	28.2	17.0	12.1	29.1
15	30	6.4	1.4	7.8	6.4	2.2	8.6
15	29	4.3	0.4	4.7	4.3	0.9	5.2
14	32	1.7	-	1.7	1.8	0.4	2.2
14	31	1.3	-	1.3	1.3	-	1.3
14	30	24.1	5.9	30.0	23.6	9.3	32.9
14	29	15.2	2.2	17.4	14.7	4.6	19.3

Table IV: Cross Sections (>1.0 mb) for all Products (Cont'd)

Z	A	250. MeV/N			400. MeV/N		
		FIRESTREAK 2	STOCHASTIC $E_o = 65$ MeV	TOTAL	FIRESTREAK 2	STOCHASTIC $E_o = 85$ MeV	TOTAL
14	28	25.0	3.6	28.6	24.1	8.0	32.1
14	27	4.8	0.5	5.3	4.9	0.9	5.8
14	26	3.1	1.4	4.5	3.0	0.4	3.4
13	29	1.9	-	1.9	1.7	0.4	2.1
13	28	1.8	-	1.8	1.9	-	1.9
13	27	14.3	1.4	15.7	14.9	2.9	17.8
13	26	4.0	-	4.0	3.8	0.5	4.3
13	25	3.8	-	3.8	3.7	-	3.7
12	26	17.3	0.7	18.0	17.0	2.1	19.1
12	25	11.9	-	11.9	12.1	0.9	13.0
12	24	25.8	0.7	26.5	25.9	1.6	27.5
12	23	4.6	-	4.6	4.6	-	4.6
12	22	3.4	-	3.4	3.5	-	3.5
11	23	11.1	-	11.1	11.2	-	11.2
11	22	2.9	-	2.9	2.9	-	2.9
11	21	3.0	-	3.0	3.0	-	3.0
10	22	10.6	-	10.6	10.8	-	10.8
10	21	8.4	-	8.4	8.6	-	8.6
10	20	18.7	-	18.7	18.6	-	18.6
10	18	2.3	-	2.3	2.2	-	2.2
9	19	3.8	-	3.8	3.9	-	3.9
8	18	3.4	-	3.4	3.4	-	3.4
8	17	2.3	-	2.3	2.4	-	2.4
8	16	4.8	-	4.8	4.7	-	4.7

Figure Legends

Fig. 1 Formation cross sections for various gamma transitions in product nuclei from 400 MeV/N ^{12}C bombardment of natural calcium. The abscissa is the minimum excitation energy of ^{40}Ca required to form the product. This figure was supplied by Dr. T. Shibata from his work of ref. 1.

Fig. 2 Cross sections for first-excited (2+) to ground (0+) transitions in various even-even products from ^{12}C on Ca at two different energies. The 250 MeV/N data are shown as relative cross sections, since the absolute normalization was not determined. The abscissa ϵ_{\min} is the same as in Fig. 1. The straight lines are a visual fit to the data points. This figure is from ref. 1.

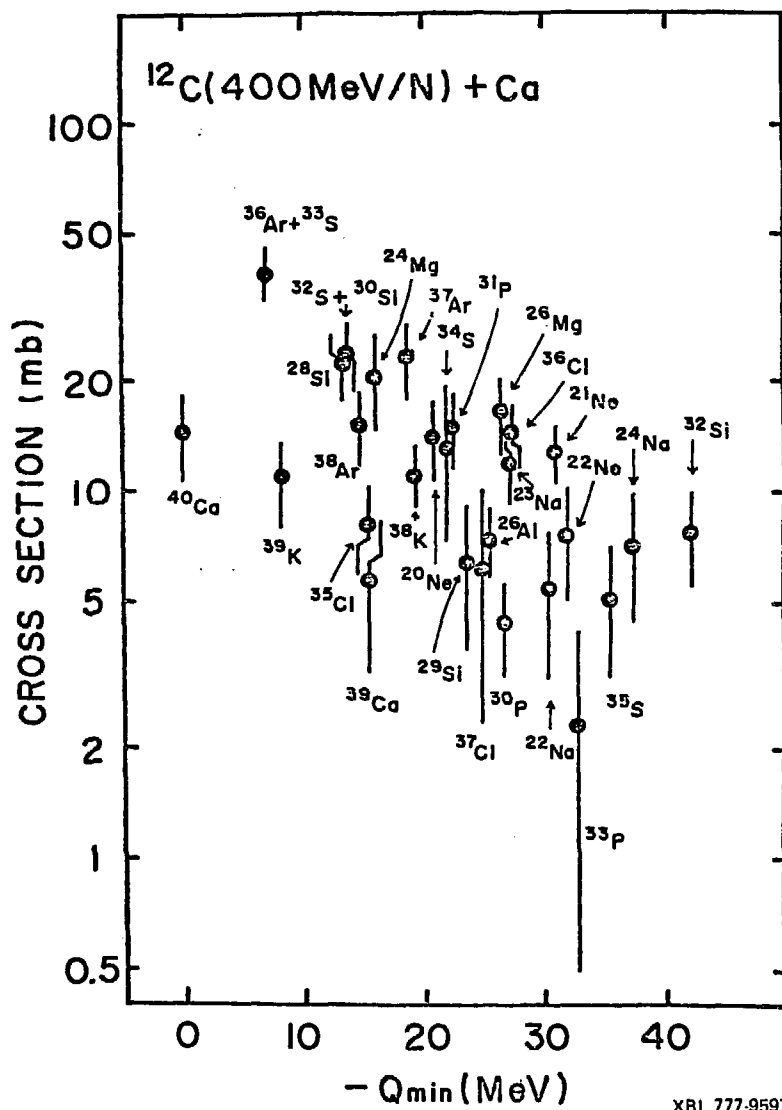


Fig. 1

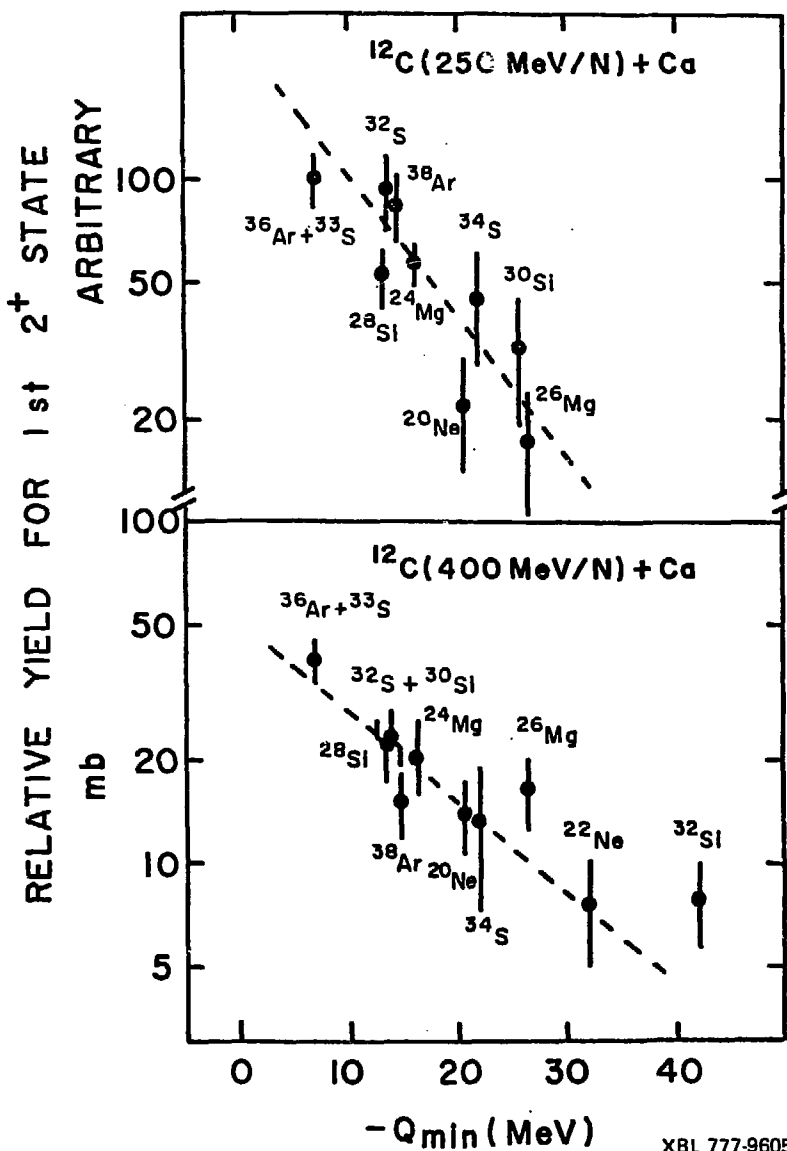


Fig. 2

XBL 777-9605